Structural Studies of Poly(1*H*,1*H*-fluoroalkyl α-fluoroacrylate)s by Infrared Spectroscopic Analysis

Tetsuo Shimizu,*,† Yoshito Tanaka,† Machie Ohkawa,‡ Shoichi Kutsumizu,‡ and Shinichi Yano‡

Research & Development Department, Daikin Industries, Ltd., Settsu, Osaka 566, Japan, and Department of Chemistry, Faculty of Engineering, Gifu University, Yanagido, Gifu 501-11, Japan

Received June 6, 1995; Revised Manuscript Received January 16, 1996⊗

ABSTRACT: IR spectral studies were performed for poly(1*H*,1*H*-fluoroalkyl α-fluoroacrylate)s $[-\{CH_2\text{-}CFC(O)OCH_2(CF_2)_nY\}_p-$, Y = H or F, $n = 1-11$] in a wide temperature range. The carbonyl absorptions [ν(C=O)] split into two peaks near 1770 ± 4 (ν_1) and 1795 ± 4 (ν_2) cm^{-1}. The ratio in absorbances of ν_2 to ν_1 increased with increasing crystalline region formed by the main chains but was independent of that formed by the fluoroalkyl side chains. The present IR results revealed that both the main and fluoroalkyl side chains participate in the formation of crystallites, but in the shorter fluoroalkyl homologoues with $n < 7$, the main chains including C=O groups in the esters mainly form the crystallites, while in the longer fluoroalkyl homologues the side chains predominate over the main chains to form the crystallites, although an ordering of main chains still exists. Moreover, the C=O bonds were considered to be in *cis* conformation to αC−F bonds in the main chain crystallites and almost in a perpendicular direction to the main chains.

Introduction

Poly(fluoroalkyl α-substituted acrylate)s (denoted hereafter PX-H*m*-F*n*-Y as illustrated in Figure 1) are comb polymers functionalized with fluoroalkyl side chains. The fluoroalkyl side chains are frequently packed in layers to form crystallites.[1−6] The structure of crystallites is much influenced by the length and chemical structure of the fluoroalkyl side chains and by the α-substituent of the acrylate moiety. Poly(fluoroalkyl acrylate)s (PH-H*m*-F*n*-Y) and poly(fluoroalkyl methacrylate)s (PM-H*m*-F*n*-Y) have been reported to form crystallites in which the fluoroalkyl side chains are arranged in layers only when the number of CF_2 moieties (n) in the fluoroalkyl side chains is larger than or equal to 7.[2,3] According to recent work for PX-H2-F8-F,[4,6] the side chain crystallites consist of a double-layer packing of the side chains at room temperature for PA-H2-F8-F and both single- and double-layer packings for PM-H2-F8-F, respectively. As temperature increases, the layer packings disappear above T_m. In our X-ray studies of a series of poly(fluoroalkyl α-fluoroacrylate)s (PF-H*m*-F*n*-Y),[5,6] however, we found that PF-H1-F*n*-Y homologues crystallize even in the shorter fluoroalkyl homologues than the $n = 4$. In the shorter fluoroalkyl homologues ($n < 7$), not only the fluoroalkyl side chains are arranged to form crystallites with a double-layer structure but also the main backbone chains are highly ordered.[5] The longer fluoroalkyl homologues (PF-H*m*-F*n*-Y, where $m = 1$ or 2 and $n \geq 7$) have crystallites with a single-layer packing at room temperature. As temperature increases, the single-layer packing tends to transform into a double-layer packing. In the longer fluoroalkyl homologues, the packing of the long side chains governs the structure of crystallites, but the main backbone chains are ordered to some extent in the crystallites and this ordering disturbs the side chain packing to produce the single-layer packing. As temperature increases above T_g, the ordering of main backbone chains decreases, resulting in changing from the single-layer packing to the double-layer packing.[6]

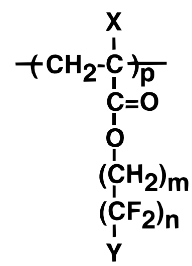

Figure 1. Chemical structure of polymers represented by PX-H*m*-F*n*-Y, where X on the polymer main chain denotes H if X = A, CH_3 if X = M, and F if X = F. m is the number of CH_2 moieties, n is the number of CF_2 moieties, and Y = F or H.

The unique structure and transformation of crystallites draw our attention toward studying the physical properties and structure of PF-Hm-F*n*-Y homologues. The present work concerns infrared (IR) spectroscopic studies of poly(1*H*,1*H*-fluoroalkyl α-fluoroacrylate)s (PF-H1-F*n*-Y) to clarify the structure of the crystallites. The splitting of the characteristic stretching vibration band of the C=O group is found to be closely connected with the structure of the crystallites.

Experimental Section

PX-H1-F*n*-Y were prepared by a radical polymerization of the corresponding monomers in 1,3-bis(trifluoromethyl)benzene, using azobis(isobutyronitrile) (AIBN) as an initiator and a chain-transfer agent as a molecular weight regulator, according to the same procedure described previously.[5,6] The polymer samples used here are listed with several physical properties in Table 1. Weight-average molecular weights (M_w) were determined by gel permeation chromatography, using THF as solvent and polystyrene as a standard. However, we were unable to determine the M_w values of PF-H1-F7-F, PF-H1-F8-F, PF-H1-F9-F, PF-H1-F11-F, and PM-H1-F8-F, because of their insolubility in THF, but their sheet samples were so tough that we may assume these are polymeric materials. ^{19}F-NMR spectra of the α-fluoroacrylate polymers were recorded on a Bruker AC-300P ^{19}F-NMR spectrometer (282.4 MHz) at room temperature, using acetone as solvent and

† Daikin Industries, Ltd.
‡ Gifu University.
⊗ Abstract published in *Advance ACS Abstracts,* April 1, 1996.

S0024-9297(95)00789-3 CCC: $12.00

Table 1. List of Polymers Used

polymers	triad tacticity[a] *mm*	*mr*	*rr*	$M_w \times 10^{-5}$	T_g/K	T_m/K	ΔH_m/(kJ mol^{-1})
PF-H1-F1-F	0.13	0.49	0.37	2.6	383	487	1.3
PF-H1-F2-H	0.12	0.47	0.41	2.2	359	449	0.41
PF-H1-F2-F	0.12	0.48	0.40	1.8	370	493	3.51
PF-H1-F7-F	0.12	0.48	0.40	ND[b]	ND	454	4.77
PF-H1-F8-F	0.13	0.46	0.41	ND	ND	458	5.32
PF-H1-F9-F	0.12	0.45	0.43	ND	ND	469	6.02
PF-H1-F11-F	0.11	0.47	0.42	ND	ND	472	7.73
PM-H1-F1-F	0.07	0.41	0.52	3.5	354		
PM-H1-F2-F	0.06	0.40	0.54	2.8	353		
PM-H1-F8-F	0.06	0.40	0.54	ND	329	362	3.6
PA-H1-F2-F	0.03	0.60	0.37	2.3	260		

[a] *mm*, isotactic; *mr*, heterotactic; *rr*, syndiotactic. [b] ND, not determined.

$CFCl_3$ as an internal standard, while we used a JEOL FX-100 ^{19}F-NMR spectrometer (93.7 MHz) to measure the ^{19}F-NMR spectra of the insoluble polymer samples in the molten state, using trifluoroacetic acid as an internal standard. The triad tacticities (*mm*, *mr*, *rr*) were obtained from the *mm*, *mr*, and *rr* peaks in the αC−F region according to the assignment of Majumder and Harwood.[7] The triad tacticities of the methacrylate polymers were obtained from the *mm*, *mr*, and *rr* peaks in the αC−CH_3 region, according to the assignment of Bovey and Tiers,[8] where ^{1}H-NMR spectra were measured on a Bruker AC-300P ^{1}H-NMR spectrometer (300 MHz) at room temperature, using acetone-d_6 as solvent and TMS as an internal standard. For poly(2,2,3,3,3-pentafluoropropyl acrylate) (PA-H1-F2-F), the triad tacticity was measured from the splitting of the ^{13}C-NMR peaks of the C=O bond, according to the assignment of Hatada,[9] using a Bruker AC-300P. Differential scanning calorimetric (DSC) data were measured at a heating rate of 10 K min^{-1} by use of a Perkin-Elmer DSC-7.

IR spectral data were recorded with a Perkin-Elmer 1640 FT-IR spectrometer, where each trace was taken as the average of 16 scans at a resolution of 4 cm^{-1}. The sheet samples were prepared mostly by cooling at a rate of about 0.3 K min^{-1} after compression-molding at the temperature of the molten state. The sheet was sandwiched between two KBr windows and then placed in a heated cell controlled within 0.5 K by use of a temperature controller (S. T. Japan, 0019-201), where each temperature was detected by a calibrated Fe−constantan thermocouple in a hole drilled in the KBr window. The oriented sheets were obtained by drawing uniaxially 2−4 times at a temperature above T_g. The anisotropic IR spectra were measured by setting them parallel and perpendicular to a KRS-5 polarizer, respectively.

Results and Discussion

Figure 2 shows IR spectra in the wavenumber range from 1500 to 2000 cm^{-1} for PX-H1-F2-F as typical examples. In all the samples, there are observed carbonyl stretching vibration peaks of the fluoroalkyl esters [ν(C=O)], but the ν(C=O) bands shift to higher wavenumbers in the order of CH_3, H, and F of the α-substituents (X). In carbonyl compounds, the ν(C=O) peaks are well known to shift to higher wavenumbers, as the electron-withdrawing effect of the α-substituent is larger. These shifts of ν(C=O) by the α-substitution seem to hold in the present crystalline and polymeric system. It is to be noted that in PF-H1-F2-F, the ν(C=O) band splits into two peaks, ν_1(C=O) at lower wavenumber and ν_2(C=O) at higher wavenumber.

Figure 3 shows the ν(C=O) bands for different PF-H1-F*n*-Y and PM-H1-F*n*-Y homologues. The splittings of ν(C=O) bands are observed in all PF-H1-F*n*-Y. To date, these splittings have been found for poly(alkyl α-chloroacrylate)s[10] and poly(methyl α-fluoroacrylate)s.[11]

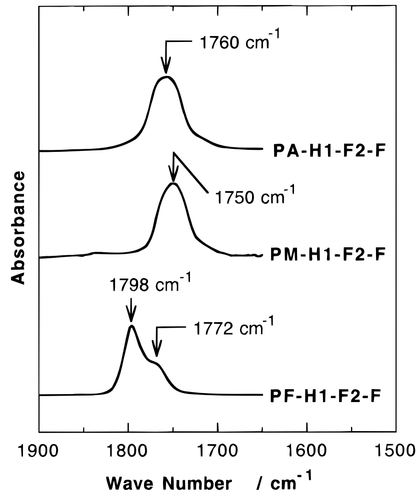

Figure 2. Carbonyl region of FT-IR spectra of PX-H1-F2-F at room temperature.

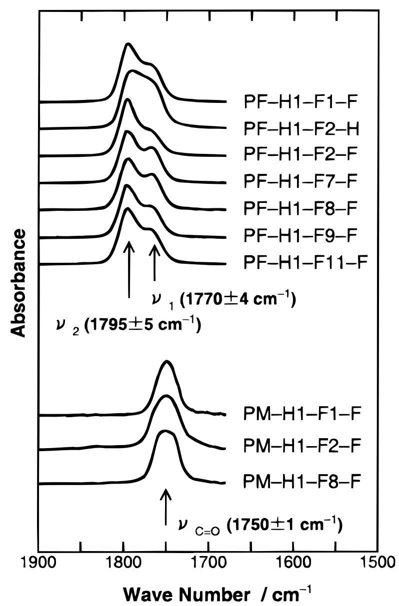

Figure 3. Carbonyl region of FT-IR spectra of PF-H1-F*n*-Y and PM-H1-F*n*-Y homologues at room temperature.

For the poly(alkyl α-chloroacrylate)s, Wesslén and Lenz assigned the splitting to a conformational (rotational) isomerism between the C=O and αC−Cl bonds, according to the assignment of Bellamy and Williams[12] for α-chloro ketone compounds; the electrostatic repulsion between C=O and αC−Cl is increased when C=O is in *cis* conformation to αC−Cl, and the ν(C=O) peaks move to higher wavenumbers, resulting in splittings of the ν(C=O) bands. Moreover, they pointed out that the fraction of *cis*-conformational sequences in the rotational isomers should depend on the stereoregularity, and isotactic polymers prefer to take *cis* conformation rather than syndiotactic polymers. This interpretation for the splitting was experimentally evidenced for poly(alkyl α-chloroacrylate)s by Dever et al.,[13] where the ratio of absorbance for ν_2(C=O) ($A_{\nu 2}$) to that for ν_1(C=O) ($A_{\nu 1}$), $A_{\nu 2}/A_{\nu 1}$, increased almost in proportion to the fraction of isotactic sequences. In Figure 3, the value of $A_{\nu 2}/A_{\nu 1}$ appears to be different among the PF-H1-F*n*-Y homologues, although the stereoregularity is almost the same among all the homologues (see triad tacticities in Table 1). Therefore, the splittings are not explained only by the stereoregularity. Figure 4A shows the temperature dependence of ν(C=O) for PF-H1-F2-F. The ν(C=O)

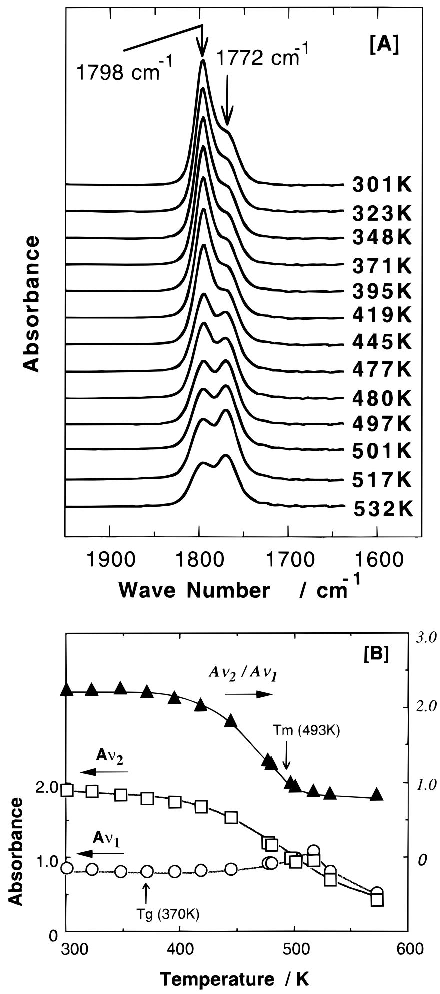

Figure 4. (A) Carbonyl region of FT-IR spectra of poly(2,2,3,3,3-pentafluoropropyl α-fluoroacrylate) (PF-H1-F2-F) at various temperatures. (B) Absorbances of ν_1(C=O) at 1772 cm^{-1} ($A_{\nu1}$) and ν_2(C=O) at 1798 cm^{-1} ($A_{\nu2}$), and the ratio ($A_{\nu2}/A_{\nu1}$) as a function of temperature.

splits into ν_1(C=O) at ~1772 cm^{-1} and ν_2(C=O) at ~1798 cm^{-1}, independent of temperature, but the value of $A_{\nu2}/A_{\nu1}$ appears to be temperature dependent; with increasing temperature, $A_{\nu2}$ considerably decreases and $A_{\nu1}$ changes little. $A_{\nu1}$, $A_{\nu2}$, and $A_{\nu2}/A_{\nu1}$ are plotted against temperature in Figure 4B. As temperature increases, $A_{\nu2}$ begins to decrease near T_g and rapidly decreases near T_m and $A_{\nu1}$ abruptly decreases above T_m. The rapid decreases of $A_{\nu1}$ and $A_{\nu2}$ above T_m may artificially take place due to a melt-flowing of sheets, but $A_{\nu2}/A_{\nu1}$ should faithfully reflect the change of ν(C=O) bands with temperature. Parts A and B of Figure 5 show variations of $A_{\nu2}/A_{\nu1}$ with temperature for PF-H1-Fn-Y and PM-H1-Fn-F homologues, respectively, with their DSC heating curves. As the temperature approaches T_m, the value of $A_{\nu2}/A_{\nu1}$ rapidly decreases, falling, above T_m, to about 0.8, independent of the homologues. In the short fluoroalkyl PF-H1-Fn-Y homologues (n = 1,2), the values of $A_{\nu2}/A_{\nu1}$ and the magnitude of decrease appear to be connected with the crystallinity, i.e., heats of fusion (ΔH_m) (in Table 1, ΔH_m is 1.3, 0.41, and 3.51 kJ mol^{-1} for PF-H1-F1-F, PF-H1-F2-H, and PF-H1-F2-F, respectively). In PF-H1-F8-F, however, ΔH_m has the large value of 5.32 kJ mol^{-1} (see Table 1) but the value of $A_{\nu2}/A_{\nu1}$ and the magnitude of decrease are comparatively small. Figure 5B shows the temperature dependences of $A_{\nu(C=O)}$ for PM-H1-F2-F and

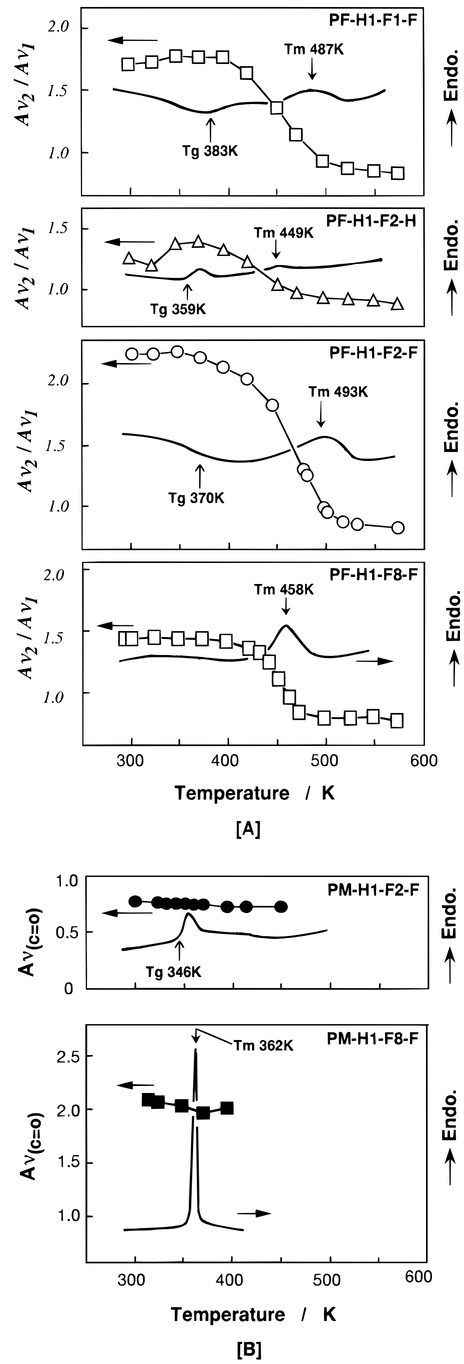

Figure 5. Temperature dependences of $A_{\nu2}/A_{\nu1}$ for PF-H1-Fn-Y (A) and $A_{\nu(C=O)}$ for PM-H1-Fn-Y (B), with DSC heating curves.

PM-H1-F8-F, in which the ν(C=O) bands do not split at all, as seen in Figure 3. The values of $A_{\nu(C=O)}$ show no temperature dependence and scarcely change near T_g or T_m. Figure 6 shows plots of $A_{\nu2}/A_{\nu1}$ versus ΔH_m (in kJ mol^{-1}) for all PF-H1-Fn-Y homologues including several samples prepared by different annealing conditions. Apparently, the plots are divided into two curves, one is for the shorter fluoroalkyl homologues (n = 1,2) and the other is for the longer fluoroalkyl homologues ($n \geq 7$). As mentioned in the Introduction, our previous X-ray work revealed that the crystallites in the shorter fluoroalkyl homologues (n = 1−4) consist of main backbone chains and fluoroalkyl side chains but the main backbone chains are predominantly packed to form the crystallites, while in the longer fluoroalkyl homologues, the fluoroalkyl side chains play a signifi-

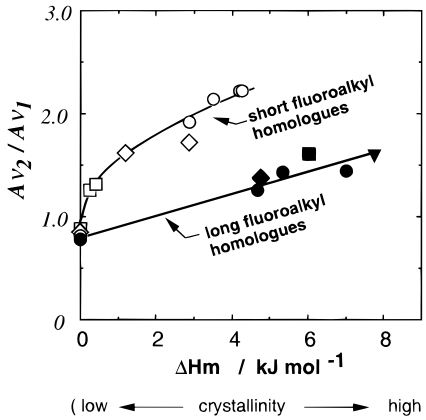

Figure 6. Relationship between $A_{\nu 2}/A_{\nu 1}$ values at room temperature and heats of fusion (ΔH_m in kJ mol^{-1}): (◊) PF-H1-F1-F; (□) PF-H1-F2-H; (○) PF-H1-F2-F; (♦) PF-H1-F7-F; (●) PF-H1-F8-F; (■) PF-H1-F9-F; (▼) PF-H1-F11-F.

cant role in forming the crystallites, although the main backbone chains are also ordered to some extent. In PH-H1-F*n*-Y and PM-H1-F*n*-Y homologues, on the other hand, it has been found that the shorter fluoroalkyl homologues are noncrystalline and in the long fluoroalkyl homologues, the fluoroalkyl side chains are arranged to form the crystals but the main backbone chains do not show any ordering. The values of ΔH_m observed in long fluoroalkyl PF-H1-F*n*-Y homologues would include the enthalpy changes for both meltings of the ordered main backbone and the fluoroalkyl side chains. The increase of $A_{\nu 2}/A_{\nu 1}$ with ΔH_m is much larger for the short fluoroalkyl homologues than for the long fluoroalkyl homologues and, moreover, the ν(C=O) does not split at all for PM-H1-F8-F, which means $A_{\nu 2}/A_{\nu 1}$ = 0, independent of ΔH_m. Referring to the X-ray diffraction results, therefore, we conclude that the value of $A_{\nu 2}/A_{\nu 1}$, which depends substantially on $A_{\nu 2}$, is closely connected with the degree of ordering of the main backbone chains in the crystallites. In PF-H1-F*n*-Y homologues, the main backbone chains are ordered together with the C=O groups of the esters in the crystallites, and the C=O groups incorporated into the crystallites are preferentially in *cis* conformation to the αC−F bonds, which results in strengthening the higher frequency band ($A_{\nu 2}$). It is important to learn that the main backbone chains are ordered in the crystallites, even in the longer fluoroalkyl PF-H1-F*n*-Y homologues. The splittings of the ν(C=O) bands found in the melts of PF-H1-F*n*-Y, whose values of $A_{\nu 2}/A_{\nu 1}$ are approximately 0.8 for all the homologues (Figure 5A), may be dependent on their stereoregularity.

Figure 7 shows polarized IR spectra for the uniaxially drawn PF-H1-F2-F and PM-H1-F2-F sheets, where ∥ and ⊥ mean IR spectra measured when the drawing direction is parallel to the polarizer and perpendicular to the polarizer, respectively. In PF-H1-F2-F, both the ν_1(C=O) and ν_2(C=O) bands are anisotropic and are larger perpendicular (⊥) to the polarizer than parallel (∥) to the polarizer, but the ν(C=O) band for PM-H1-F2-F is isotropic. In other words, the drawn PF-H1-F2-F sheet has a perpendicular dichroism but the drawn PM-H1-F2-F shows no dichroism. The isotropy of PM-H1-F2-F convinces us again that PM-H1-F2-F is noncrystalline. In Figure 8, the dichroic ratio is plotted against the uniaxially drawing ratio for ν_1(C=O) and ν_2(C=O) in the drawn PF-H1-F2-F sheet, where the dichroic ratio is defined as $A_{\parallel}/A_{\perp}$. The dichroic ratio increases with increasing draw ratio for both the ν_1(C=O) and ν_2(C=O) bands, but the magnitude of the increase is larger for the ν_2(C=O) band than the ν_1(C=O) band. This dichroism was observed for all the uniaxially drawn PF-H1-F*n*-Y homologues used here. Our previous X-ray work revealed that the uniaxially drawing increases the degree of crystallinity and that the main backbone chains are arranged in a parallel direction to the drawing direction and the fluoroalkyl side chains are ordered in a perpendicular direction to the main backbone chains. The perpendicular dichroism for the two ν(C=O) bands indicates that the C=O groups are packed together with the main backbone chains in the crystallites and the C=O bonds are almost in a perpendicular direction to the main backbone chains.

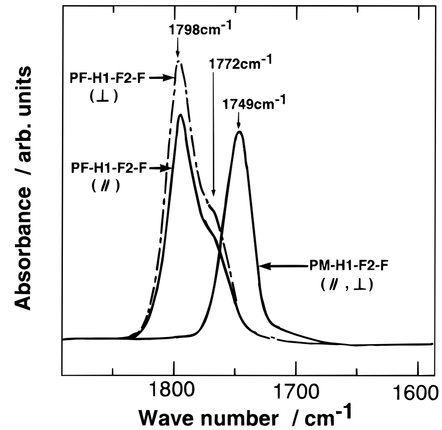

Figure 7. Polarized IR spectra for uniaxially drawn PF-H1-F2-F and PM-H1-F2-F sheets when the drawing direction is parallel (∥) or perpendicular (⊥) to the polarizer.

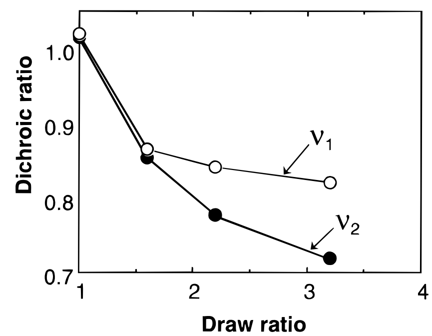

Figure 8. Plots of dichroic ratio versus draw ratio for uniaxially drawn PF-H1-F2-F sheets.

Conclusion

From the present IR spectral studies, we obtained the following results on the structure of crystallites in PF-H1-F*n*-Y. In the shorter fluoroalkyl homologues (n < 7), the main backbone chains are predominantly ordered together with the C=O groups of the esters to form crystallites, while in the longer fluoroalkyl homologues ($n \geq 7$), the fluoroalkyl side chains are predominantly packed together to form crystallites but an ordering of the main backbone chains also exists. It is to be emphasized that C=O bonds incorporated into the ordered main backbone chain region are predominantly in *cis* conformation to αC−F bonds, and the C=O bonds are almost in a perpendicular direction to the main backbone chains in the crystallites.

Acknowledgment. We very much thank Dr. S. Koizumi (Mitsuboshi Co. Ltd., Osaka, Japan) and

Professor Dr. K. Tadano (Gifu College of Medical Technology, Gifu, Japan) for helpful discussions. S.K. wishes to acknowledge the support of the Ministry of Education, Science, and Culture, Japan (Grant-in-Aid for Scientific Research No. 05750800).

References and Notes

(1) Pittman, A.; Ludwig, B. *J. Polym. Sci.* **1969**, *7*, 3053.
(2) Budovskaya, L. D.; Ivanova, V. N.; Oskar, L. N.; Lukasov, S. V.; Baklagina, Yu. G.; Sidorovich, A. V.; Nasledov, D. M. *Vysokomol. Soedin., Ser. A* **1990**, *32*, 561.
(3) Okawara, A.; Maekawa, T.; Ishida, Y.; Matsuo, M. *Polym. Prepr. Jpn.* **1991**, *40*, 3898.
(4) Volkov, V. V.; Platé, N. A.; Takahara, A.; Kajiyama, T.; Amaya, N.; Murata, Y. *Polymer* **1992**, *33*, 1316.
(5) Shimizu, T.; Tanaka, Y.; Kutsumizu, S.; Yano, S. *Macromolecules* **1993**, *26*, 6694.
(6) Shimizu, T.; Tanaka, Y.; Kutsumizu, S.; Yano, S. *Macromol. Symp.* **1994**, *82*, 173; *Macromolecules*, in press.
(7) Majumder, R. N.; Harwood, H. J. *Polym. Bull.* **1981**, *4*, 391.
(8) Bovey, F. A.; Tiers, G. V. D. *J. Polym. Sci.* **1960**, *44*, 173.
(9) Hatada, K. *Kobunshi* **1981**, *30*, 696.
(10) Wesslén, B.; Lenz, R. W. *Macromolecules* **1971**, *4*, 20.
(11) Pittman, C. U., Jr.; Ueda, M.; Iri, K.; Imai, Y. *Macromolecules* **1980**, *13*, 1031.
(12) Bellamy, L. J.; Williams, R. L. *J. Chem. Soc.* **1957**, 4294.
(13) Dever, G. R.; Karasz, F. E.; MacKnight, W. J.; Lenz, R. W. *J. Polym. Sci., Polym. Chem. Ed.* **1975**, *13*, 2151.

MA950789B